Mikulewitsch, Merlin ; Auerswald, Matthias Marcus ; von Freyberg, Axel ; Fischer, Andreas

Geometry Measurement of Submerged Metallic Micro-Parts Using Confocal Fluorescence Microscopy

Journal Article as: peer-reviewed accepted version (Postprint)

DOI of this document*(secondary publication): https://doi.org/10.26092/elib/3309

Publication date of this document: 13/09/2024

* for better findability or for reliable citation

Recommended Citation (primary publication/Version of Record) incl. DOI:

Mikulewitsch, M., Auerswald, M.M., von Freyberg, A. et al. Geometry Measurement of Submerged Metallic Micro-Parts Using Confocal Fluorescence Microscopy. Nanomanuf Metrol 1, 171–179 (2018). https://doi.org/10.1007/s41871-018-0019-6

Geometry Measurement of Submerged Metallic Micro-Parts Using Confocal Fluorescence Microscopy

Merlin Mikulewitsch[1] · Matthias Marcus Auerswald[1] · Axel von Freyberg[1] · Andreas Fischer[1]

Abstract
The in situ geometry measurement of microstructures in the laser chemical machining (LCM) manufacturing process places high demands on measurement systems because the specimen is submerged in a closed fluid circuit. The steep slopes of the manufactured micro-components and the general lack of accessibility hinder the use of standard techniques such as tactile measurement or conventional confocal microscopy. A technique based on confocal fluorescence microscopy shows promise for increasing the measurability on metallic surfaces with large curvatures. By applying an intensely scattering fluorescent coating to the specimen, the surface position can be determined by the change in fluorescence signal at the boundary between specimen and coating. In contrast to the currently tested thin coatings ($<100\,\mu m$) the measurements in layers thicker than 1 mm, as required for in situ application at the LCM process, show distinct dependencies on the fluorescent medium in terms of concentration and index of refraction. Hence, a fundamentally different signal evaluation approach based on a physical model of the fluorescence signal is needed to extract the surface position information from the detected fluorescence intensity signal. For the purpose of validation, the measurement of a step geometry is performed under the condition of a thick fluid layer and referenced with a tactile measurement. As a result, the model-based approach is shown to be suitable to detect the geometry parameter step height with an uncertainty of 8.8 µm for a step submerged in a fluid layer with a thickness of 2.3 mm.

Keywords Laser chemical machining · Micro-manufacturing · In situ metrology · Confocal fluorescence microscopy · Geometry measurement

1 Introduction

1.1 Motivation

The manufacturing of metallic microstructures is a task of increasing importance in engineering that places high demands on manufacturing processes in terms of dimensional accuracy as well as operational efficiency and production throughput. Manufacturing processes such as µEDM, micro-milling or laser ablation are established techniques in this field, but suffer from high cost, tool wear or induced thermal stress, respectively [1, 12]. Laser chemical machining (LCM) is a promising alternative process that allows for inexpensive manufacturing of microstructures in hard metals, such as dies for microforming [18], without heat damage or structural alterations to the material [2]. The material removal is based on the laser-induced thermo-chemical reaction between an etchant fluid and the submerged workpiece metal, with the removal being strictly limited to the laser-affected area [9]. Thus, laser chemically machined geometries can reach structure sizes between 10 and 400 µm, depending on the laser-focus diameter, with steep slopes and a surface roughness of up to 0.3 µm [14]. The fluctuating process environment however, caused by chaotic thermal interactions between fluid and workpiece geometry, complicates the determination of optimal process parameters to produce a desired geometry [19]. To avoid time-intensive preliminary experiments, a closed-loop quality control has been designed to improve both the manufacturing speed and quality of laser chemical

✉ Merlin Mikulewitsch
m.mikulewitsch@bimaq.de

[1] University of Bremen, Bremen Institute for Metrology, Automation and Quality Science (BIMAQ), Linzer Str. 13, 28359 Bremen, Germany

machining [18]. The current post-process measurement closes the control loop but necessitates removing the workpiece from the production line after each manufacturing step [18]. This disturbance of the process environment and the elapsed time between the next manufacturing step creates undesirable deviations of process parameters for the following control iteration. Thus, to improve the feasibility and acceptance of laser chemical machining as a competitive manufacturing process, the development of an in situ measurement method is paramount.

1.2 State of the Art

The challenging conditions of the LCM process, such as the requirement that the workpiece has to be submerged in a closed fluid circuit, hinder the in situ application of many measurement methods. The general lack of accessibility to the workpiece for instance, makes the use of tactile geometry acquisition impractical, demonstrating the need for contactless measurement methods based on optical acquisition. Established micro-topography measurement techniques can be separated into interferometric methods (e.g., displacement interferometry [3, 4], digital holography, etc.) and other techniques [4], such as conventional laser-scanning confocal microscopy, light sheet microscopy or HiLo microscopy [11]. However, these techniques are still hindered by the in situ conditions, such as process-induced currents, thermal gradients and refractive index fluctuations for the case of interferometric methods [3, 18], or high surface angles for the case of conventional confocal microscopy [5]. For the application in environments where the surface of the measured object is completely covered by a fluid medium, a novel method based on the confocal detection of the fluorescence emitted by the fluid shows promise as an in situ measurement technique. The topography measurement is based on detecting the boundary position of the specimen surface and the fluid through the change in fluorescence signal, while the confocal detection volume is scanned vertically through the fluid (cf. Sect. 2). Since it does not detect the light reflected at the surface like conventional confocal techniques, but rather the light emitted by the fluorophore covering it, light is detected even under angles $> 75°$ from the surface normal [8]. Thus, even a measurement of specimen with sharp edges and high surface angles is possible [4, 5], while still offering a lateral resolution comparable to conventional confocal microscopy. Previous applications employed this technique to the measurement of metallic micro-spheres with high curvatures by coating the specimen surface with a thin fluorescent film $< 100\,\mu m$ to [5] increase the amount of scattered light. This reduced the otherwise occurring edge-artifacts and improved the measurement in comparison to conventional confocal microscopy where the purely reflective approach falls short. Another application utilized the suitability of this method for in situ measurement on processes where a fluid is inherently present, to detect the tool wear of a cutting tool edge thinly covered ($< 113\,\mu m$) by a fluorescent cutting fluid [7, 15]. In contrast to existing works, the in situ conditions of the LCM process entail neither such a thin liquid layer nor a thinly deposited fluorophore film (with a size of 0.1–10 µm) [5, 8], but a thicker liquid layer (typically in range of 0.1–10 mm) in which the measured object is completely submerged. The fluorescence signal in thicker fluid layers exhibits substantial dependencies on factors like fluorophore concentration, surface reflectivity and index of refraction that could not be observed in the applications in thin fluid layers. Therefore, the development of an signal processing method for accurate geometry acquisition is necessary, based on a physical model of the fluorescence signal that considers these effects. This approach needs to be verified in order to confirm the validity of the physical model and show the suitability of the confocal fluorescence microscopy for the measurement in thick fluid layers that meet the in situ conditions of the LCM process.

1.3 Aim and Outline of the Article

This article aims to demonstrate the suitability of confocal fluorescence microscopy to measure micro-geometries submerged in thick fluid layers $> 100\,\mu m$. For this purpose, the step height of a submerged step geometry is measured using a model-based signal evaluation approach and subsequently compared to a tactile reference measurement of the same parameter. The measurement principle and experimental setup of the confocal fluorescence microscopy method are described in Sects. 2 and 3. Further, the signal processing methods and evaluation strategy for detecting the surface position of microstructures with confocal fluorescence microscopy are outlined in Sect. 4. The experimental results are discussed and verified in Sect. 5. The article closes with a conclusion in Sect. 6.

2 Measurement Principle

The principle of measurement as shown in Fig. 1 is based on the detection of fluorescence intensity emitted from the fluid covering the specimen using a confocal microscopy setup (cf. Fig. 2). The confocal principle prevents light not originating from a volume around the focus of the objective (*confocal volume*) from contributing to the detected fluorescence signal. Scanning the confocal volume of the excitation laser vertically (in z-direction) through the fluorescent fluid produces a characteristic fluorescence intensity signal (Fig. 1 left), also known as the depth

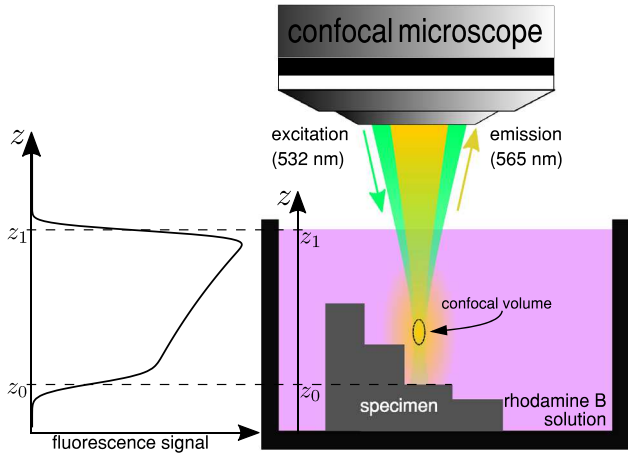

Fig. 1 Principle of the confocal fluorescence microscopy-based measurement technique: scanning the focus of the confocal volume axially through the fluid produces a fluorescence intensity signal (left) only for positions z of the confocal volume inside the fluid. For thick fluid layers, the Lambert–Beer law of absorption manifests as an exponential decay of the fluorescence signal

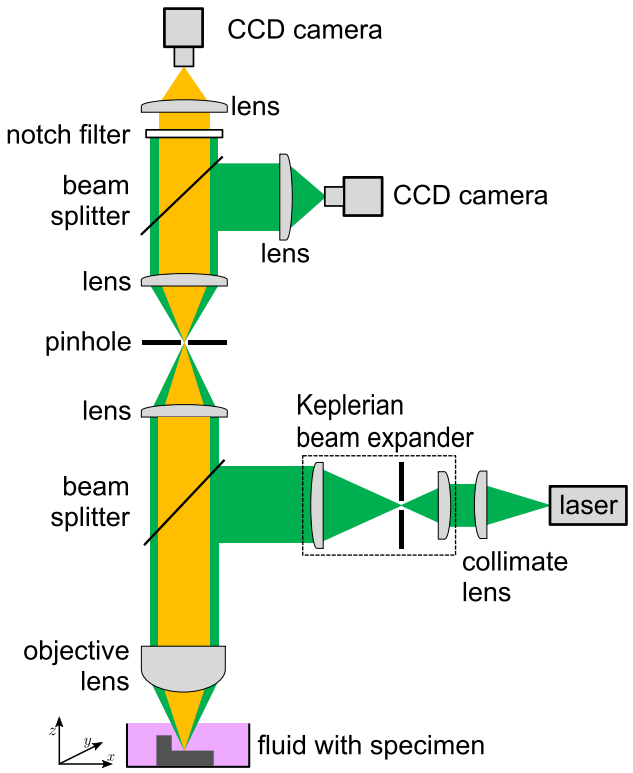

Fig. 2 Schematic diagram of the confocal fluorescence microscopy setup, with excitation light (green) and fluorescence light (yellow)

response. Since the excitation light is filtered out, only light that is emitted by the fluid inside the confocal volume is detected. For values of z far outside the boundaries of the fluid $(z_0 < z < z_1)$, no signal is produced since the confocal volume is located either in air or the specimen, where no fluorescent fluid is present to generate light. The signal does not decay abruptly at the boundary, but gradually, depending to the vertical extent of the confocal volume. In fact, the exact surface position z_0 correlates with the inflection point of the fluorescence intensity signal when the confocal volume is moved from inside the surface upwards. As such the determination of z_0 is not trivial, opposed to very thin fluid layers, where the depth response is more similar to that of conventional confocal microscopy where the intensity peak corresponds to the surface position. For the case of thicker fluid layers, the properties of the fluorescence signal depend strongly on the fluorophore concentration and the fluid depth. With high fluorophore concentrations or thick fluid layers, the Lambert–Beer law of absorption causes less excitation light to reach far into the fluid, resulting in the decay of the fluorescence signal before the confocal volume reaches the specimen surface. This effect is negligible for thin fluid layers, but needs to be taken into consideration while choosing the fluorophore concentration for measurements in thicker layers. For the purpose of understanding the fluorescence signal generation, a physical model of the fluorescence signal is developed in Sect. 4.1.

3 Experimental Setup

The measurement arrangement of the confocal fluorescence microscopy is shown in Fig. 2. A green diode laser with a wavelength of $\lambda = 532\,\text{nm}$ is introduced to the optical system after passing a Keplerian beam expander, which adjusts the beam diameter to the aperture of the remaining optical system. The light is redirected by a beam splitter to the objective lens (NA = 0.42, WD = 20 mm) exciting the fluid surrounding the measured object. The fluorescent fluid consists of an aqueous solution of Rhodamine B in which the measured object lies completely submerged within a petri dish. The specimen can be positioned using a 3-axis linear stage (cf. Fig. 3) to enable a scanning of the laser focal position through the fluid. The light emitted by the fluid, consisting of both the fluorescence ($\lambda = 565\,\text{nm}$) as well as the scattered excitation light ($\lambda = 532\,\text{nm}$), is collected by the objective lens. After passing back through the beam splitter and it is focused on a pinhole (aperture diameter: 5 µm) that attenuates light originating far from the focal plane, thus producing the confocal effect. Behind the pinhole, a notch filter with a center wavelength of 532 nm and a full width at half maximum (FWHM) of 17 nm is used to separate the excitation light from the fluorescence light which is ultimately detected by a charge-coupled device (CCD). By setting up a beam splitter behind the pinhole, a second CCD was utilized to detect the reflected excitation signal and observe the diffraction pattern behind the pinhole to

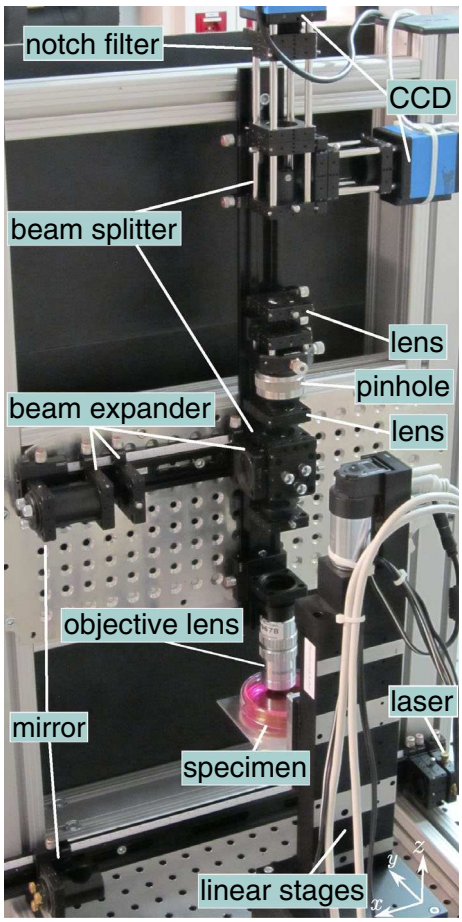

Fig. 3 Photograph of the experimental setup of the confocal fluorescence microscopy

simplify the adjustment of the optical arrangement. Thus, the depth response of the confocal microscope was calibrated using a plane mirror to achieve a FWHM of 30 µm. This parameter determines the extent of the confocal volume in z-direction, while the lateral resolution (theoretical value for the objective: 1.54 µm) determines its lateral extent. The fluorescence intensity signal is acquired by the CCD (sum over all illuminated pixels) while scanning the confocal volume in z-direction through the fluid in 10 µm steps. The measurement is performed point-wise in y-direction to acquire points along a line perpendicular to the step of the submerged reference object in 0.25 mm steps. With an exposure time of up to 300 ms, the signal acquisition for the vertical scan through the fluid for a single point along the line of measurement was up to 6 minutes. Since the determination of the surface position from the measured signal is not a simple peak detection as for conventional confocal microscopy based on the acquisition of reflected light, a more complex signal processing scheme is necessary. To incorporate the underlying effects of the fluorescence signal generation, a physical model is devised in Sect. 4.1, with which the surface position can be determined using suitable evaluation methods.

4 Signal Processing Methods

4.1 Fluorescence Model

For the purpose of modeling the fluorescence signal, the confocal volume in which it is generated needs to be described first. The spatial distribution of the confocal volume intensity can be characterized in a first approximation by a three-dimensional Gaussian function [10, 13]

$$I(\boldsymbol{r},z) = I_0 \cdot \mathrm{e}^{-\frac{2}{\omega_0^2}\left(r^2+\frac{z^2}{\kappa^2}\right)}, \quad \text{with } \boldsymbol{r} = \begin{pmatrix} x \\ y \end{pmatrix}. \tag{1}$$

e^{-2} width of this distribution is denoted by ω_0 in xy-direction and by $\kappa \cdot \omega_0$ in z-direction, scaled by a constant factor κ dependent on the detection pinhole of the confocal setup. It usually holds that $\kappa > 1$, since the confocal volume is in general much broader in z-direction. Since the detected light is generated by the fluid and the confocal microscope only detects light from inside the confocal volume, the signal rapidly decreases if this volume moves outside the fluid. The fluorescent fluid can therefore be regarded as a weighting factor, that is zero outside its boundaries, determining the intensity generated in the confocal volume. To get the detected fluorescence intensity signal (cf. Fig. 1, left) an integration over the total confocal volume needs to be performed. Thus, the fluorescence intensity I_F detected at position z can be derived by convolving the total horizontal intensity of the confocal volume $\int_{-\infty}^{\infty} I(\boldsymbol{r},z)\mathrm{d}\boldsymbol{r}$ in vertical direction with an exponential weighting function $\eta(z)$, representing the Lambert–Beer law of absorption inside the fluorophore [6]:

$$I_\mathrm{F}(z) = \eta(z) * \int_{-\infty}^{\infty} I(\boldsymbol{r},z)\mathrm{d}\boldsymbol{r}, \quad \eta(z) = \begin{cases} \mathrm{e}^{\varepsilon\cdot(z-z_1)} & z_0 \le z \le z_1 \\ 0 & \text{otherwise} \end{cases} \tag{2}$$

With the substitution of $I(\boldsymbol{r},z)$ from Eq. (1) in Eq. (2), the fluorescence intensity function I_F is given by

$$\begin{aligned} I_\mathrm{F}(z) &= I_0 \cdot \int_{z_0}^{z_1}\int_{-\infty}^{\infty} \mathrm{e}^{\varepsilon\cdot(\tilde{z}-z_1)} \cdot \mathrm{e}^{-\frac{2}{\omega_0^2}\left(\tilde{\boldsymbol{r}}^2-\frac{(z-\tilde{z})^2}{\kappa^2}\right)}\mathrm{d}\tilde{\boldsymbol{r}}\mathrm{d}\tilde{z} \\ &= \frac{I_0\pi^{3/2}\omega_0^2\xi}{4}\mathrm{e}^{\varepsilon\cdot(z-z_1)+\varepsilon^2\xi^2} \cdot \left(\operatorname{erf}\left(\frac{z-z_0}{2\xi}+\varepsilon\xi\right)\right. \\ &\quad \left. -\operatorname{erf}\left(\frac{\hat{z}-z_1}{2\xi}+\varepsilon\xi\right)\right) + \text{const} \quad \text{with } \xi = \frac{\kappa\omega_0}{2\sqrt{2}}. \end{aligned} \tag{3}$$

The fluorescence intensity function takes the form of a difference of two Gaussian error functions weighted by the exponential decay of the Lambert–Beer law. Equation (3) is the basis for the model function $f(z)$, with the parameters A, C, ϵ, Ξ, z_0 and z_1, that is used to describe the fluorescence intensity with respect to the axial displacement z:

$$f(z) = A\left[\operatorname{erf}\left(\frac{z-z_0}{2\Xi}+\epsilon\Xi\right) - \operatorname{erf}\left(\frac{z-z_1}{2\Xi}+\epsilon\Xi\right)\right]\cdot \mathrm{e}^{\epsilon(z-z_1)} + C \tag{4}$$

The surface position z_0 is then determined by fitting the model function $f(z)$ to the measured fluorescence intensity data using a Levenberg–Marquardt nonlinear least squares algorithm. Performing this fit for each point-wise acquired fluorescence signal, the surface geometry of the specimen is acquired.

4.2 Refractive Index Correction

The measured surface positions are distorted by the light of the confocal volume passing through the interface between two media with different refractive indices. The actual focal position is shifted from its nominal position due to the refraction-caused change in beam angle at the interface fluid/air (see Fig. 4), causing the position of the confocal volume to be underestimated. This systematic deviation of the measured position data needs to be corrected in order to obtain a valid measurement.

Assuming that the focal shift is only determined by the marginal rays of the aperture [16, 17], the following relation can be derived by the geometrical considerations depicted in Fig. 4:

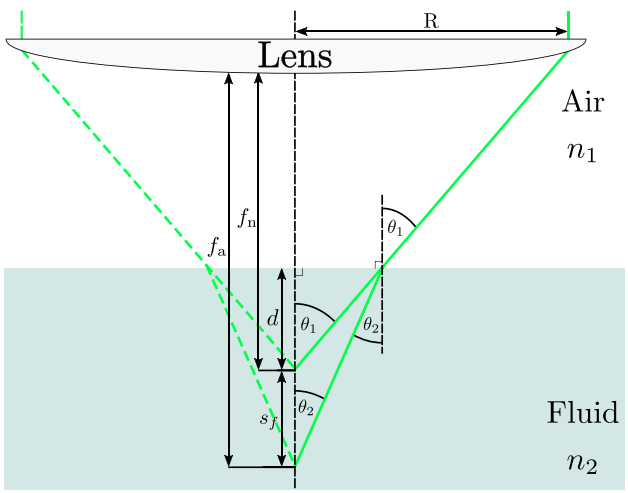

Fig. 4 Optical scheme demonstrating the focal shift s_f caused by the refractive index mismatch between air and the fluorescent fluid. The objective lens focuses the incident light an actual distance f_a rather than the nominal focusing distance f_n

$$\frac{\tan\theta_2}{\tan\theta_1} = \frac{f_a - f_n + d}{d} \tag{5}$$

With $\tan\theta_1 = \frac{R}{f_n}$, the focal shift $s_f = f_a - f_n$ can be determined by rearranging Eq. (5) and applying Snell's law:

$$\begin{aligned} s_f(d) &= d\cdot\frac{\tan\theta_2}{\tan\theta_1} - d \\ &= d\cdot\frac{f_n}{R}\tan\sin^{-1}\left(\frac{n_1}{n_2}\sin\tan^{-1}\left(\frac{R}{f_n}\right)\right) - d \end{aligned} \tag{6}$$

The change in focal shift $\Delta s_f = s_f(d_1+\Delta z) - s_f(d_1)$, when the focus is moved by Δz from some position d_1 is then the linear relation

$$\Delta s_f = \frac{n_1}{n_2}\frac{1}{\sqrt{1+\frac{R^2}{f_n^2}-\left(\frac{n_1 R}{n_2 f_n}\right)^2}}\cdot\Delta z = \frac{\Delta z}{\gamma}. \tag{7}$$

Using the relation $\frac{R}{f_n} = \tan\sin^{-1}\mathrm{NA}$, equation (7) can also be expressed in terms of NA as

$$\Delta s_f = \frac{n_1}{n_2}\frac{\sqrt{1-\mathrm{NA}^2}}{\sqrt{1-\left(\frac{n_1}{n_2}\mathrm{NA}\right)^2}}\cdot\Delta z = \frac{\Delta z}{\gamma}, \tag{8}$$

provided the incident beam takes up the total area of the objective lens, which constitutes an upper limit to the focal shift. Since this is not necessarily the case in reality, the real focal shift factor γ_{real} is often smaller and needs to be determined first. By dividing the measured positional data by the factor γ, the focal shift can be corrected. Since the focal shift effect causes the apparent position to be underestimated by a factor of up to three (depending on the numerical aperture of the objective lens) in watery solutions [16], a correction of this effect is imperative for accurate measurements of submerged micro-geometries.

5 Results

The fluorescence light created by the focused excitation laser inside the fluid is shown in Fig. 5. The confocal volume used to scan the surface of the submerged object has a vertical spread around the focus of about 20–30 µm and has as such no directly visible boundaries.

To correct the distortion of the measured surface geometry caused by the focus shift, the real focal shift factor γ_{real} (cf. Eq. 7) is measured first. For this purpose, the height of a step geometry was measured by confocally acquiring the light reflected from a mirror placed on two adjacent steps, first in air and then submerged in fluid. The measurement was performed for several points along a line perpendicular to the edges of the step geometry, with a lateral linear stage step size of 0.5 mm. Note that the data

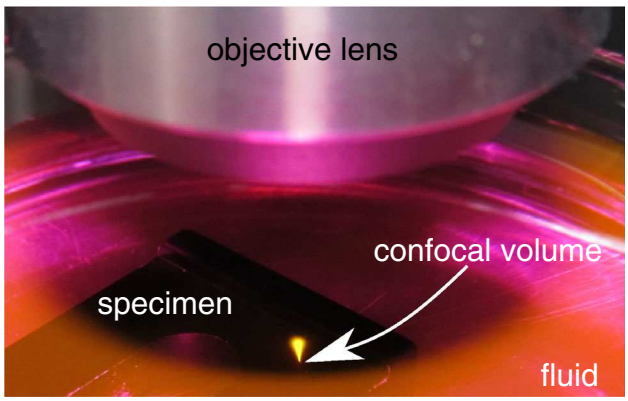

Fig. 5 Photograph of the petri dish filled with the fluorescent fluid. The fluorescence (565 nm) is exited by the excitation laser (532 nm—not visible) and is focused on a specimen submerged in the fluid

shown in Fig. 6 do not originate from the light emitted by the fluid but the excitation light which is reflected by a flat mirror. The height h of the step was in both cases determined by measuring the confocal depth response with a vertical linear stage step size of 2 µm and an exposure time of 0.1 ms. The lateral position of the peak that corresponds to the mirrors surface is shown in Fig. 6 for fluid and air on the right side, respectively. Since the surface of the step is tilted with respect to the coordinate system of the linear stages, the determination of the step height was performed according to the method detailed in standard ISO 5436-1. In order to correct the tilt, first a linear regression is performed on the points of the lower surface and subtracted from the total data. The step height h is then determined by taking the mean of the points on the upper step surface with respect to the tilt-corrected lower surface. The disparity between the two measured heights h_{air} and h_{fluid} shown in Fig. 6 can be traced back to the difference of refractive index between fluid and air, resulting in a focus shift that distorts the fluid data. The focal shift factor γ_{real} to correct the measured positional data is thus the ratio of the two heights

$$\gamma_{\text{real}} = \frac{h_{\text{air}}}{h_{\text{fluid}}} = \frac{535.7\,\mu\text{m}}{312.2\,\mu\text{m}} = 1.72\,. \tag{9}$$

By multiplying γ_{real} with the surface position z_0 of the fluorescence intensity signal, the influence of the fluid on the determined position is compensated. The measurement using the fluorescence signal was performed over a step along a line oriented perpendicular to the edges of the step, on a step object (nominal step height: 250 µm) submerged in fluid with a maximal depth of 2.3 mm. Because the specimen surface has a relatively high reflectivity, fluorescence light is reflected from the specimen surface into the confocal volume, causing a change to the fluorescence signal that is not considered in the present model. To avoid the detection of this light, the specimen was tilted slightly ($<25°$) in the direction parallel to the edge of the steps. The fluorescence intensity signal, shown blue in Fig. 7 for one point on the specimen, was acquired with a vertical linear stage step size of 10 µm and an exposure time of 30 ms. By fitting the fluorescence intensity model $f(z)$ (see Eq. 4) to the measured data (shown black in Fig. 7), the

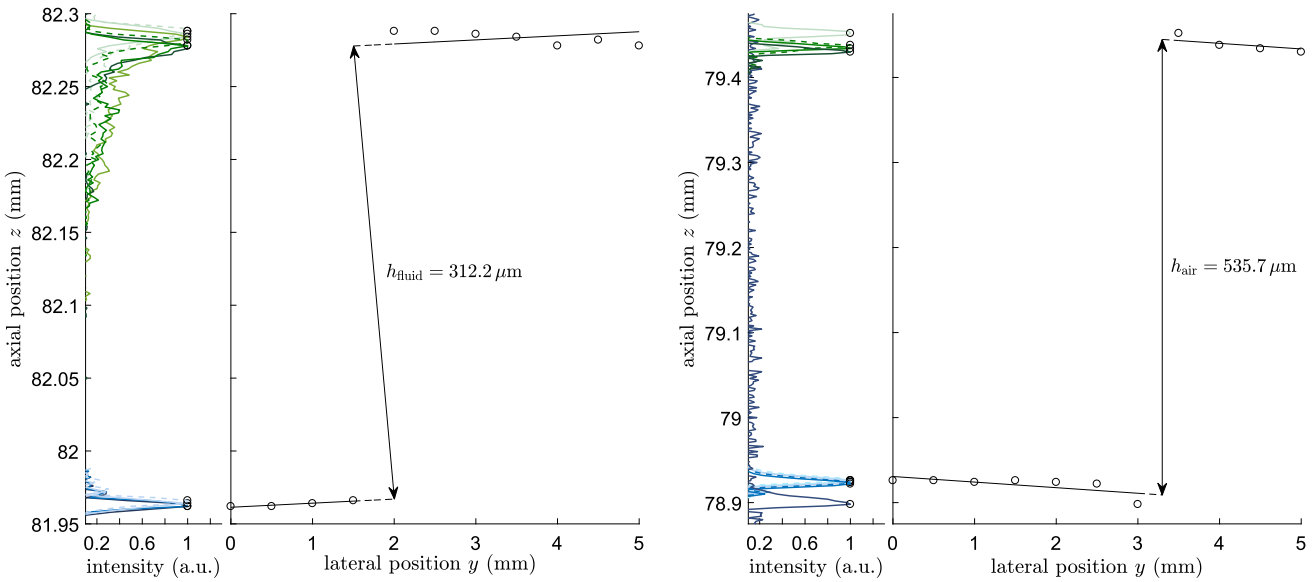

Fig. 6 For the determination of the real focal shift factor γ_{real}, the step height h of two mirrors placed on adjacent steps was measured in fluid (left) and air (right), respectively. The confocal depth responses of the reflected excitation light along a lateral displacement perpendicular to the step edge are shown on the left, while the determined peak positions corresponding to the surface positions are shown on the right, respectively

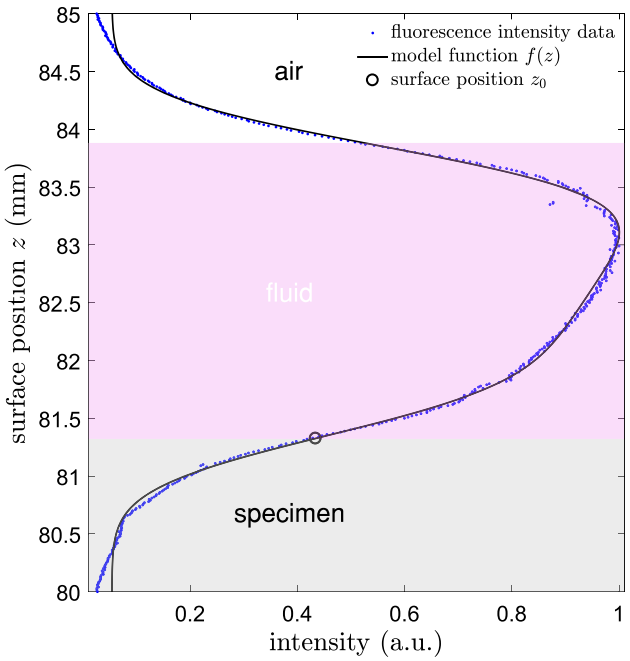

Fig. 7 Fluorescence intensity data (blue dots) and fitted model function $f(z)$ (black line) for one point on the specimen. The surface position z_0 resulting from the fit is marked as a circle

surface position z_0 was determined. The boundary conditions and start values for the fit parameters A, C, ϵ, Ξ, z_0 and z_1 were chosen heuristically according to an approximate determination of the fluid boundaries, since an automatic determination of these values is not yet implemented.

As shown in Fig. 7, the fit corresponds well with the measured data (goodness of fit $R^2 \approx 0.99$), but for points far outside the fluid (such as at $z = 85\,\text{mm}$) the model deviates from the acquired signal. This constitutes a source of uncertainty for the measured surface positions and step heights, because the fitting model does not consider all parameters of influence. To ameliorate this effect a threshold was set, outside of which the points were excluded from the fit, improving the surface position determination but providing a further source of uncertainty. The results of the surface positions z_0 determined by the fit are shown in Fig. 8 for each point along the measured line. To determine the step height h of a step, the same approach previously used for the measurement of the focal shift factor in Fig. 6 has to be performed, because the submerged step geometry is also tilted with respect to the linear stages. The two outliers are disregarded from the measurement as an edge artifact and are not considered for the step height determination. The linear regression was performed on the lower step surface and all z_0 were corrected to this level so that the step height could be determined by subtracting the mean over all points of the lower from the mean over all points of the upper step surface:

$$h = \overline{z}_{0,\text{upper}} - \overline{z}_{0,\text{lower}} = (150.5 \pm 5.1)\,\mu\text{m} \qquad (10)$$

Correcting the influence of the refracting fluid using the previously determined focal shift factor γ_{real} results in the

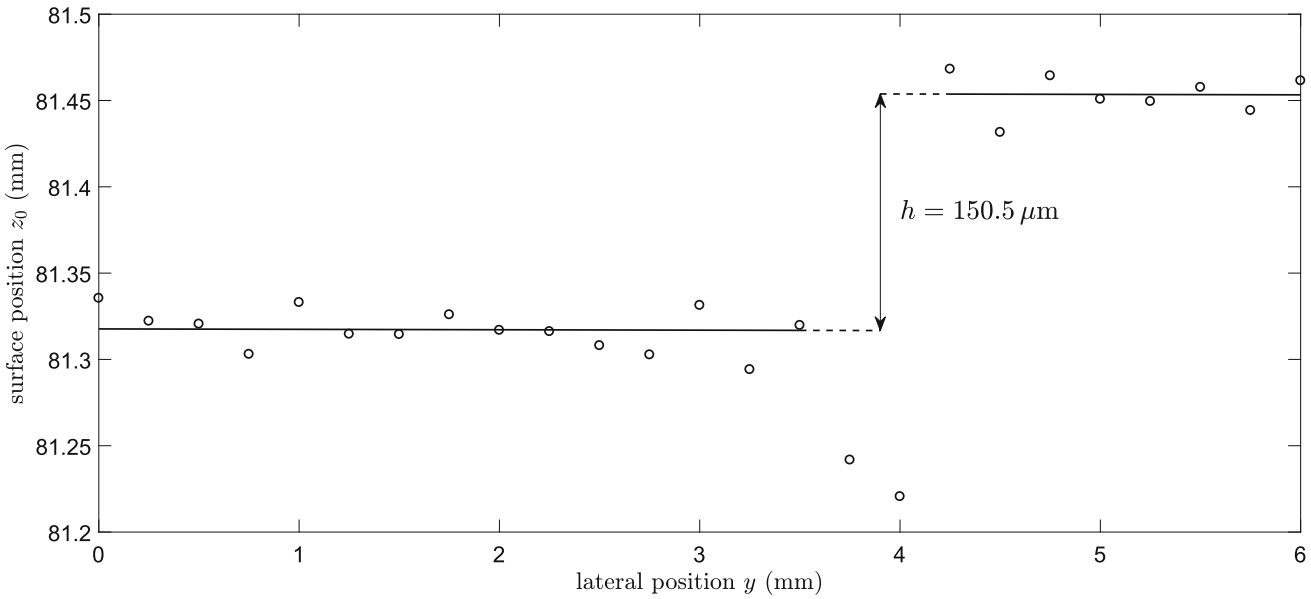

Fig. 8 Surface positions z_0 of a step from a submerged step geometry (nominal step height $(253.5 \pm 0.2)\,\mu\text{m}$) resulting from the fit of the measured data (lateral distance between points: 0.25 mm) . The step height h of the step was determined with respect to a linear regression of the lower step surface. In order to evaluate the step height measurement, the influence of the refractive fluid medium has to be corrected by multiplication with the focal shift factor γ_{real}

following value and standard deviation for the step height h:

$$h \times \gamma_{\text{real}} = (150.5 \pm 5.1)\,\mu\text{m} \times 1.72 = (258.2 \pm 8.8)\,\mu\text{m} \quad (11)$$

The points of each step surface show a relatively large spread (up to 20%), due to the general surface condition as well as uncertainties in the fitting model. The uncertainty of the measured fluorescence intensity data and a high sensitivity of the fit to starting and boundary parameters are also contributing factors. Comparing the measured and corrected step height $h = (258.2 \pm 8.8)\,\mu\text{m}$ with the reference height $h_{\text{ref}} = (253.5 \pm 0.2)\,\mu\text{m}$, which was determined using a tactile profilometer, the step height measurement shows no significant systematic deviations. The measurement is shown to be in agreement with the reference measurement within the uncertainty of 8.8 µm. The result demonstrates that while the stochastic deviations of each measured position on both step surfaces are still quite high, the determination of geometry parameters such as step height is still possible using statistical methods. As such, the fluorescence microscopy is shown to be in principle suitable for in situ measurement of geometry parameters of specimen submerged by fluids with a thicknesses exceeding 100 µm. Fully understanding the cause of the stochastic deviations contributing to the step height uncertainty as well as quantifying the uncertainty of the measured correction factor γ_{real} requires further research. To achieve the aim of a fully integrated in situ measurement system for the laser chemical machining process, the measurement uncertainty of 8.8 µm needs to be reduced further to 1 µm.

6 Conclusion

The measurements on a referenced step geometry with a nominal step height of $(253.5 \pm 0.2)\,\mu\text{m}$ show that the confocal fluorescence microscopy-based measurement technique is capable to determine the geometry parameter step height for microstructures submerged in thick fluid layers $> 100\,\mu\text{m}$. The measurement results in a step height of $(258.2 \pm 8.8)\,\mu\text{m}$ which demonstrates the suitability of the model-based approach for the step height determination in an in situ application with a 2.3 mm thick fluid layer. While no systematic deviations remain, the causes of the uncertainty of 8.8µm need to be further characterized in order to reduce it to the desired 1 µm. Further steps in improving the measurement uncertainty and subsequent geometry parameter determination will be the incorporation of the effect of surface reflectivity into the theoretical model as well as the quantification of the uncertainty of the focal shift factor. The reduction in the measurement time is also an important step toward a full in situ application.

Acknowledgements The authors gratefully acknowledge the financial support by the Deutsche Forschungsgemeinschaft (DFG, German Research Foundation) for subprojects A5 & B9 within the SFB 747 (Collaborative Research Center) "Mikrokaltumformen – Prozesse, Charakterisierung, Optimierung."

References

1. Ahmed N, Darwish S, Alahmari AM (2016) Laser ablation and laser-hybrid ablation processes: a review. Mater Manuf Process 31(9):1121–1142
2. De Silva A, Pajak P, McGeough J, Harrison D (2011) Thermal effects in laser assisted jet electrochemical machining. CIRP Ann Manuf Technol 60:243–246
3. Gerhard C, Vollertsen F (2010) Limits for interferometric measurements on rough surfaces in streaming inhomogeneous media. Prod Eng Res Dev 4(2–3):141–146
4. Hansen H, Carneiro K, Haitjema H, De Chiffre L (2006) Dimensional micro and nano metrology. CIRP Ann 55:721–743
5. Liu J, Liu C, Tan J, Yang B, Wilson T (2016) Super-aperture metrology: overcoming a fundamental limit in imaging smooth highly curved surfaces. J Microsc 261(3):300–306
6. Malzer W, KanngieSSer B (2005) A model for the confocal volume of 3d micro x-ray fluorescence spectrometer. Spectrochim Acta Part B At Spectrosc 60(9–10):1334–1341
7. Maruno K, Michihata M, Mizutani Y, Takaya Y (2016) Fundamental study on novel on-machine measurement method of a cutting tool edge profile with a fluorescent confocal microscopy. Int J Autom Technol 10(1):106–113
8. Michihata M, Fukui A, Hayashi T, Takaya Y (2014) Sensing a vertical surface by measuring a fluorescence signal using a confocal optical system. Meas Sci Technol 25(6):064004
9. Pajak P, Desilva A, Harrison D, Mcgeough J (2006) Precision and efficiency of laser assisted jet electrochemical machining. Precis Eng 30(3):288–298
10. Petersen NO (2017) Foundations for nanoscience and nanotechnology. CRC Press, Boca Raton
11. Philipp K, Smolarski A, Koukourakis N, Fischer A, Sturmer M, Wallrabe U, Czarske JW (2016) Volumetric HiLo microscopy employing an electrically tunable lens. Opt Express 24:15029–15041
12. Qin Y (ed) (2015) Chapter 1 - overview of micro-manufacturing. In: Micromanufacturing engineering and technology. Micro and nano technologies, 2nd edn. William Andrew Publishing, Boston, pp 1–33. https://doi.org/10.1016/B978-0-323-31149-6.00001-3
13. Rüttinger S, Buschmann V, Krämner B (2008) Comparison and accuracy of methods to determine the confocal volume for quantitative fluorescence correlation spectroscopy. J Microsc 232:343–352
14. Stephen A, Vollertsen F (2010) Mechanisms and processing limits in laser thermochemical machining. CIRP Ann Manuf Technol 59(1):251–254
15. Takaya Y, Maruno K, Michihata M, Mizutani Y (2016) Measurement of a tool wear profile using confocal fluorescence microscopy of the cutting fluid layer. CIRP Ann Manuf Technol 65(1):467–470
16. Visser T (1992) Refractive index and axial distance measurements in 3-d microscopy. Optik 90:17–19
17. Wang K, Wu J, Day R, Kirk TB (2012) Utilizing confocal microscopy to measure refractive index of articular cartilage. J Microsc 248(3):281–291

18. Zhang P, von Freyberg A, Fischer A (2017) Closed-loop quality control system for laser chemical machining in metal micro-production. Int J Adv Manuf Technol 93(9–12):3693–3703
19. Zhang P, Goch G (2015) A quality controlled laser-chemical process for micro metal machining. Prod Eng 9(5–6):577–583

Merlin Mikulewitsch received his M.Sc. degree in physics at the University of Bremen. Since 2016 he is working at the Bremen Institute for Metrology, Automation, and Quality Science (BIMAQ) in the group dimensional metrology to gain his Ph.D. His current research is focused towards optical micro-metrology with regards to in-situ applications in fluid environments.

Matthias Marcus Auerswald received the B.Sc. and the M.Sc. from the University of Applied Sciences Germany, in 2013 and 2015, respectively. Since 2015, he works at the Bremen Institute for Metrology, Automation and Quality Science (BIMAQ). His current research interests include the identification and characterization as well as the development of an optical measurement system for investigation the surface of large involute gears.

Axel von Freyberg received his Dipl.-Ing. degree at the University of Bremen. From 2001 until 2003 he was working as research engineer at the Bremen Institute of Industrial Technology and Applied Work Science (BIBA). Since 2003 he is head of the dimensional metrology group at the institute, which changed its name into Bremen Institute for Metrology, Automation and Quality Science (BIMAQ) in 2007. His main research topics are numerical approximation and evaluation techniques for dimensional metrology.

Andreas Fischer is Full Professor with the University of Bremen and head of the Bremen Institute for Metrology, Automation, and Quality Science (BIMAQ). He received his Ph.D. in electrical engineering at Technische Universität Dresden. His research interests include the identification, characterization, and application of measurement limits as well as the development of optical measurement systems for the investigation of dynamic flow, shape, and sur-